



Nonlinear Soil Resistance of Pile Group Foundation Subjected to Load in Different Directions Based on Nonlinear 3D FEM

T. Nakano⁽¹⁾, Y. Miyamoto⁽²⁾

⁽¹⁾ Graduate student, Graduate School of Engineering Osaka University / JSPS research fellow,
e-mail: nakano_takaharu@arch.eng.osaka-u.ac.jp

⁽²⁾ Professor, Graduate School of Engineering Osaka University, e-mail: miyamoto@arch.eng.osaka-u.ac.jp

Abstract

The stress on any given pile of a pile group foundation varies during an earthquake because the mechanisms of horizontal soil resistance differ from each other depending on the pile location. In order to calculate the seismic response of the structure supported on a pile group, a beam-spring model with nonlinearity on the subgrade reaction along the pile shafts is needed. Because the structure is subjected to a multi-directional earthquake motion, it is also necessary to obtain the relationship between the subgrade reaction and the loading direction.

In this paper, static analyses using the nonlinear three-dimensional finite element method (3D FEM) were performed to obtain the nonlinearity in the horizontal soil resistance of a pile group foundation subjected to arbitrary directional loading. Analyses were conducted on a single pile, and 2 x 2, 3 x 3, 5 x 5, 7 x 7 and 9 x 9 pile groups placed in sand and clay soil, for spacing to diameter ratios of 2.5 and 6.0. To calculate nonlinear soil springs, the piles were subjected to forced displacement in arbitrary directions including diagonal directions. In these analyses, shear force at the pile head and subgrade reaction along each pile shaft were calculated. The major findings obtained from these analyses can be summarized as follow:

- 1) The pile group effect on the subgrade reactions was larger than that of shear forces at the pile head. The number of piles and the soil type affected the pile group coefficient, while the pile displacement and its loading direction had small impact on it.
- 2) The shear force at the pile head and the subgrade reaction along the pile shaft differed depending on the pile location and became larger in the case of the front piles during the loading. These differences could be clearly observed in a pile group with narrower pile spacing in sand.
- 3) For a pile located on the edge of a pile group, the shear force at the pile head and the subgrade reaction along the pile shafts differed depending on the direction of loading. When the pile became a front pile, the shear force at the pile head and the subgrade reaction became larger. These differences could be clearly observed in the pile group with the narrower pile spacing in sand.
- 4) The hysteresis curve of the pile subgrade reaction-displacement relationship located in sand and clay had different characteristics. When the piles were placed in sand, the hysteresis of the pile located on the edge of the pile group showed an asymmetric loop, while those in the middle of the pile group were symmetrically-shaped. When placed in clay, the hysteresis of all piles showed an almost symmetric loop.

Keywords: Pile group foundation, Pile group effect, Nonlinear Soil spring, 3D FEM, Multi-directional input

1. Introduction

Pile group foundations have been severely damaged due to very large earthquakes in recent years. For example, the 1995 Hyogo-ken Nanbu (Kobe) Earthquake ^[1] and The 2011 off the Pacific coast of Tohoku Earthquake ^[2]. In these damages, it is considered that soil-pile group interaction has played an important role. A pile stress during an earthquake varies in a pile group because mechanisms of horizontal soil resistance differ depending on the pile location. Thus, in order to calculate the seismic response of a structure supported by a pile group foundation at the member-level, it is necessary to consider the different horizontal soil resistance of each pile.

Figure 1 shows a lumped mass model to calculate the response of the structure supported by a pile group. Lumped mass models are generally classified into decomposed and integrated models. The decomposed model is used to calculate the response of a superstructure and piles separately, while the integrated model is used to take both responses into consideration simultaneously. For these models, piles are modeled as beam elements with masses and horizontal soil resistance is modeled as discrete springs. When we use a decomposed model, springs at the pile head, which present the shear force-displacement relationships at the pile head, are mounted to the bottom of a superstructure. As when using an integrated model, soil springs along the pile shafts, which present the subgrade reaction-displacement relationships at each depth, are mounted to each mass in the piles. In order to calculate the response of a pile group at the member-level using a model with multi piles as shown in Figure 1b, it is crucial to appropriately set soil springs. In addition, because the structure is subjected to a multi-directional earthquake motion, it is also necessary to obtain the directivity of soil springs.

A number of studies have been conducted on the pile group effect through experimental and analytical approaches. For example, Tuzuki et al. (1992) ^[3] observed the impedance of pile groups by dynamic loading tests; Tamaki et al. (1971) ^[4] and Lemnitzer et al. (2008) ^[5] obtained the pile group coefficients by static loading tests; Kosa et al. (1998) ^[6], Suzuki et al. (2003) ^[7], Hijikata et al. (2007) ^[8] and Kashiwa et al. (2008) ^[9] experimentally observed different pile stresses at each pile in pile groups. These above studies have been mainly focused on the characteristics of springs at the pile head. On the other hand, some studies have been focused on the characteristics of soil springs along the pile shafts. For example, Miyamoto et al. (1995) ^[10] calculated soil springs along the pile shafts based on thin layer method analyses directly; Kosa et al. (1998) ^[6],

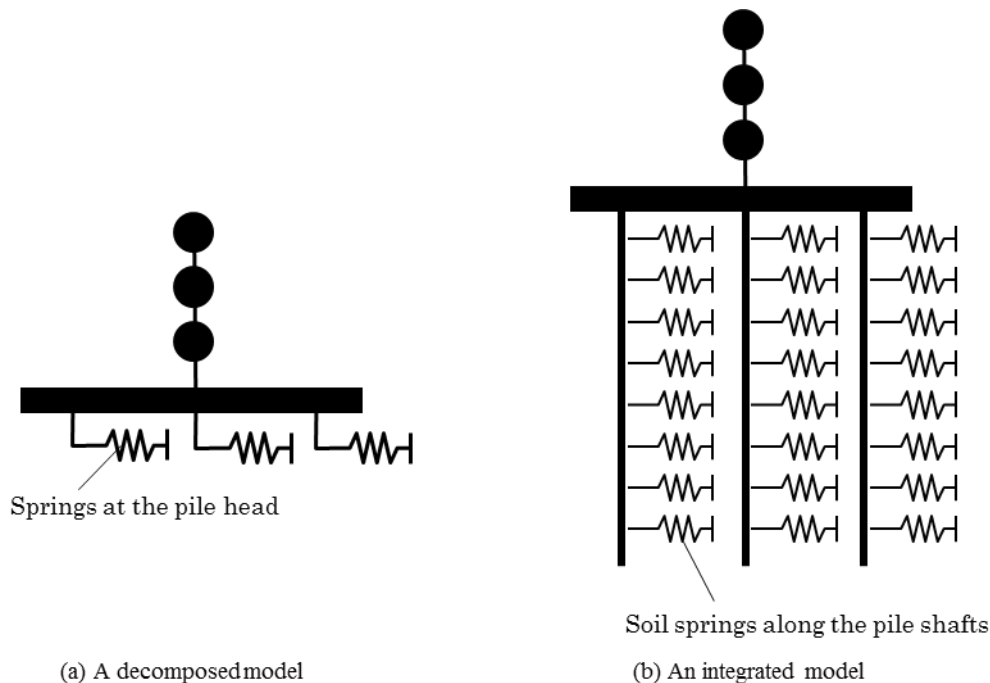


Fig. 1 – Lumped mass models of a structure supported by a pile group



Suzuki et al. (2003)^[7] and Hijikata et al. (2007)^[8] experimentally obtained subgrade reaction at each pile in pile groups; Hijikata et al. (2006-2007)^[11] analytically calculated the distribution of subgrade reaction by three-dimensional finite element method (3D FEM) analyses. These studies have demonstrated that soil springs differ from each other depending on the pile location. However, the directivity of soil springs has not been cleared.

Therefore, the main contribution of this paper is to evaluate soil springs along the pile shafts in pile groups, which are subjected to arbitrary directional loading based on static analyses using the nonlinear 3D FEM.

2. Analysis model and calculation method

Nonlinear 3D FEM analyses were conducted separately on a single pile, and 2 x 2, 3 x 3, 5 x 5, 7 x 7 and 9 x 9 pile groups with a pile spacing (S) of $2.5B$ or $6.0B$, where B was an outer diameter of the piles. To discuss the directivity of horizontal soil resistance of a pile group, a loading angle θ , an angle formed by the direction of pile displacement with X-axis (as shown in Figure 2,) was changed at 15° intervals. The piles were driven to 11 m depth into homogeneous sand or clay soil. The sand had an internal frictional angle of 31.9° and a cohesion of 1 kN/m^2 , while the clay had an internal frictional angle of 1° and a cohesion of 50 kN/m^2 . Other properties of the soil are indicated in Table 1. In order to discuss the difference of failure criterions, density, S-wave velocity and Poisson's ratio were set to same value for sand and clay. The piles were made of steel and had an outer diameter of 600 mm, a thickness of 9 mm and a length of 11 m.

Figure 2 exhibits the finite element model for the 5 x 5 pile group with a pile spacing of $2.5B$. Soil was modeled as perfect elastic-plastic bodies with Mohr-Coulomb yield criterion. The initial shear modulus of the soil was set to $0.5\rho Vs^2$, where ρ was density and Vs was shear wave velocity. For the side boundaries of the soil, horizontal displacements of nodes were restricted, while for the bottom boundary of the soil, vertical displacements of nodes were restricted. Gapping and sliding at the pile-soil interface were considered by the contact determination algorithm based on the penalty method. The coefficient of friction of the interface was set to 0.6. Monotonic and cyclic loadings are conducted under displacement control. For the monotonic loading, maximum displacement was set to 100mm, while for the cyclic loading, displacement amplitudes were set to $\pm 1\text{mm}$, $\pm 2\text{mm}$, $\pm 5\text{mm}$, $\pm 10\text{mm}$, $\pm 20\text{mm}$, $\pm 50\text{mm}$ and $\pm 100\text{mm}$ consecutively. The following sections introduce results of the monotonic loading unless otherwise specified.

Table 1 – Properties of the soil

Soil	ρ (t/m ³)	Vs (m/s)	Poisson's ratio	ϕ (deg.)	c (kN/m ²)
Sand	1.8	110	0.33	31.9	1
Clay	1.8	110	0.33	1	50

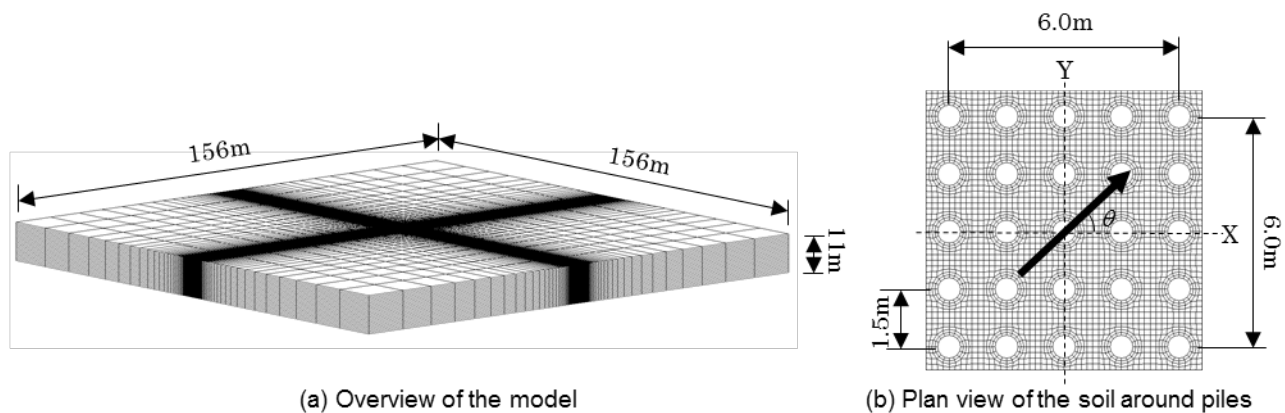


Fig. 2 – Numerical analysis model by 3D finite element (5 x 5 pile group, $S/B=2.5$)

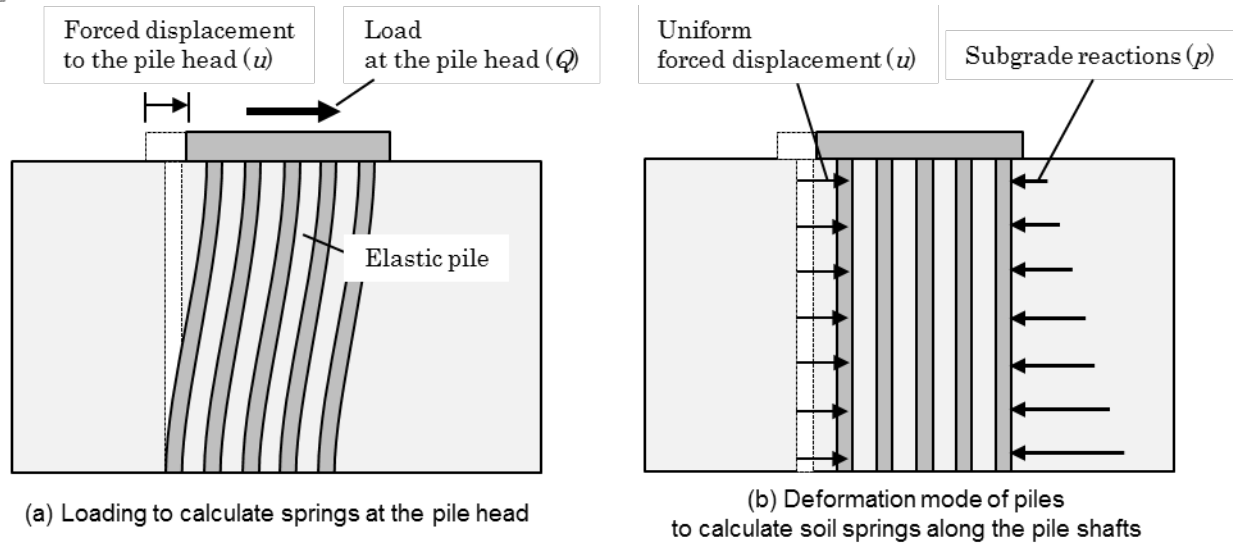


Fig. 3 – Calculation method of springs at the pile head and soil springs along the pile shafts

Springs at the pile head and soil springs along the pile shafts were calculated by the static horizontal loading analyses as illustrated in Figures 3a and 3b respectively. The force-displacement of the springs at the pile head were calculated by loading at the pile head as shown in Figure 3a. The piles were modeled as elastic shell elements. The pile heads were jointed to one rigid footing which was restricted on rotation with rigid connections. The given shear force-displacement relationship at the pile head was determined as a nonlinear load-displacement relationship of the springs at the pile head. In further analyses, the force-displacement of the soil springs along the pile shafts was obtained as shown in Figure 3b. For these analyses, the piles were modeled as rigid shell elements, and a same forced displacement was induced to all nodes in all piles. The given subgrade reaction-displacement relationship at each depth was determined as a nonlinear load-displacement relationship of the soil springs.

3. The pile group effect on springs at the pile head

The pile group coefficient of springs at the pile head is defined by the following relationship:

$$\alpha_H = \frac{\sum_i Q_i(u)}{N_p \cdot Q_S(u)} \quad (1)$$

Where $Q_i(u)$ is the shear force at the pile head of the i -th pile when reaching a displacement of u at pile head, $Q_S(u)$ is the shear force at the pile head of the single pile for the displacement u , and α_H is the pile group coefficient of the springs at the pile head.

Figure 4 shows the relationship between the coefficient α_H and the number of piles (N_p) with a pile spacing of $2.5B$. Without depending on a certain soil type and displacement and loading angle, α_H was related to N_p . The larger N_p was, the smaller α_H would become. When the piles were placed in sand, α_H would be as large as $N_p^{-0.3}$. When the piles were placed in clay, α_H would be as large as $N_p^{-0.2}$. Thus, the pile group effect was greater for the case of sand. On the other hand, the extent of the displacement of piles and the loading direction had only a small impact on α_H .

Figure 5 illustrates the distribution of shear force at the pile head for the 5 x 5 pile group with a pile spacing of $2.5B$ when subjected to a displacement of 100 mm. The shear force differed from each other depending on the pile location, and it was larger at front piles. For a loading angle of 0° , the number of the front

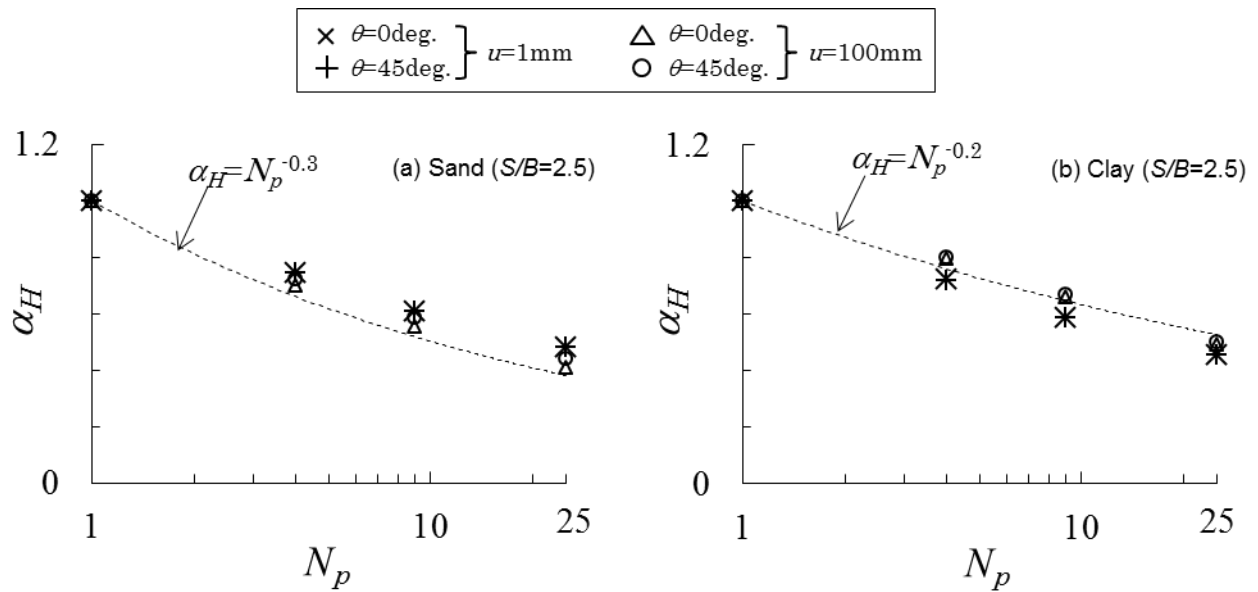


Fig. 4 – Relationship between pile group coefficient of springs at the pile head (α_H) and the number of piles (N_p)

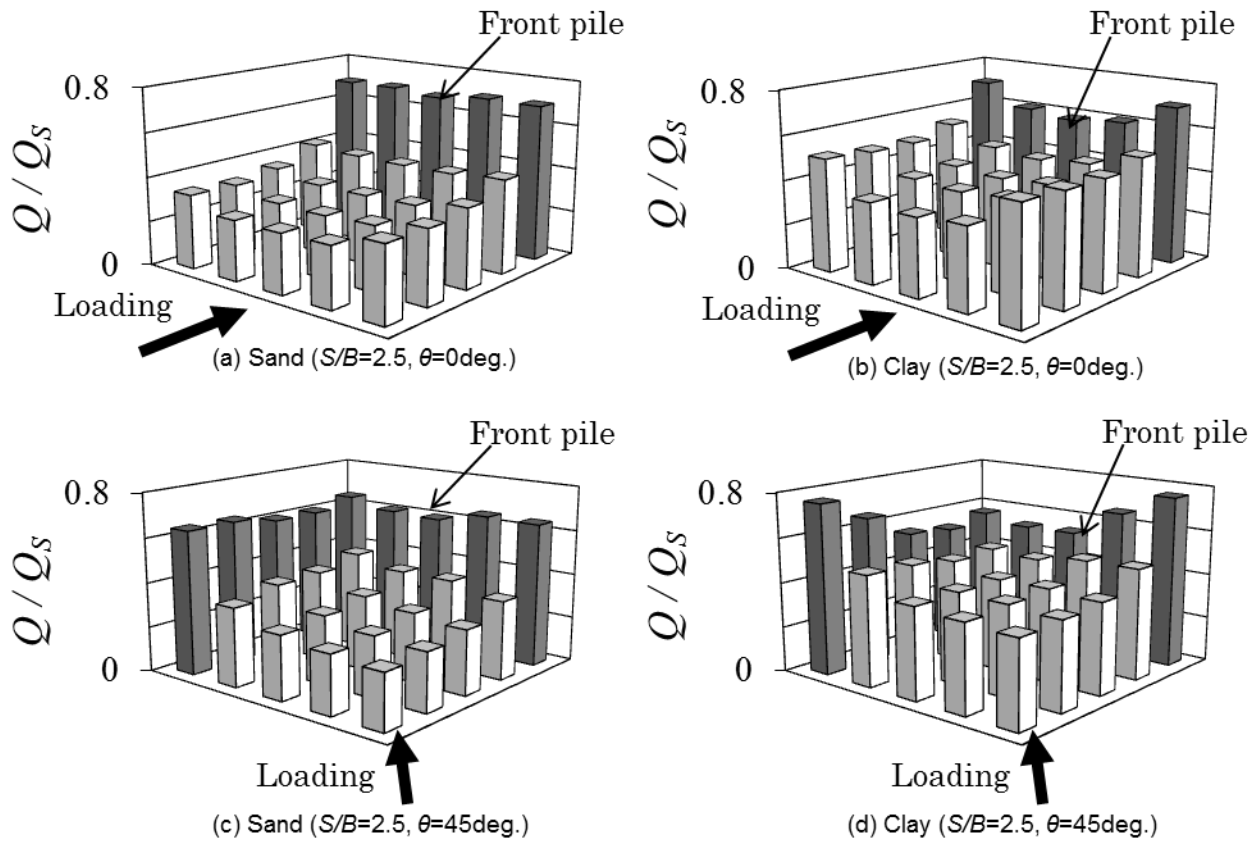


Fig. 5 – Distribution of the shear force at the pile head (5 x 5 pile group, $u=100\text{mm}$)



piles was five, while for a loading angle of 45°, there were nine front piles. Especially the difference of shear force at each pile head was demonstrated more clearly when the piles were placed in sand.

4. The pile group effect on soil springs along the pile shafts

The characteristics of shear forces at the pile head (springs at the pile head) are influenced by the characteristics of subgrade reactions (soil springs along the pile shafts.) In this chapter, soil springs are discussed.

A pile group coefficient of soil springs along the pile shafts is calculated by:

$$\beta_H = \frac{\sum_i p_i(u, z)}{N_p \cdot p_s(u, z)} \quad (2)$$

Where $p_i(u, z)$ is the subgrade reaction at depth z of the i -th pile when reaching a displacement of u , $p_s(u, z)$ is the subgrade reaction at depth z of the single pile for the displacement u , and β_H is the pile group coefficient of soil springs along the pile shafts.

Figure 6 shows the relationship between the coefficient β_H and the number of piles (N_p) at GL-1.5 m with a pile spacing of $2.5B$. Similar to the pile group coefficient of springs at the pile head, β_H was related to N_p . The larger N_p was, the smaller β_H would be become. When the piles were placed in sand, β_H would be as large as $N_p^{-0.5}$. When the piles were placed in clay, β_H would be as large as $N_p^{-0.4}$. The value of β_H was smaller than that of α_H . Therefore, the pile group effect was greater on the soil springs along pile shafts than the springs at the pile head. When comparing different displacements, the difference of β_H was small when the piles were placed in sand; when the piles were placed in clay, the value of β_H in the case of $u = 100\text{mm}$ was 1.2~2.0 times larger than the case of $u = 1\text{mm}$. Furthermore, the loading angle had small impact on β_H .

Figure 7 illustrates the distribution of the subgrade reaction at GL-1.5 m for the 5 x 5 pile group which is subjected to a displacement of 100 mm. Similar to the shear force at pile head, the subgrade reaction differed from each other depending on the pile location, and it was larger at the front piles. The difference of the subgrade reaction could be seen more clearly in a pile group with the narrower pile spacing or placed in sand.

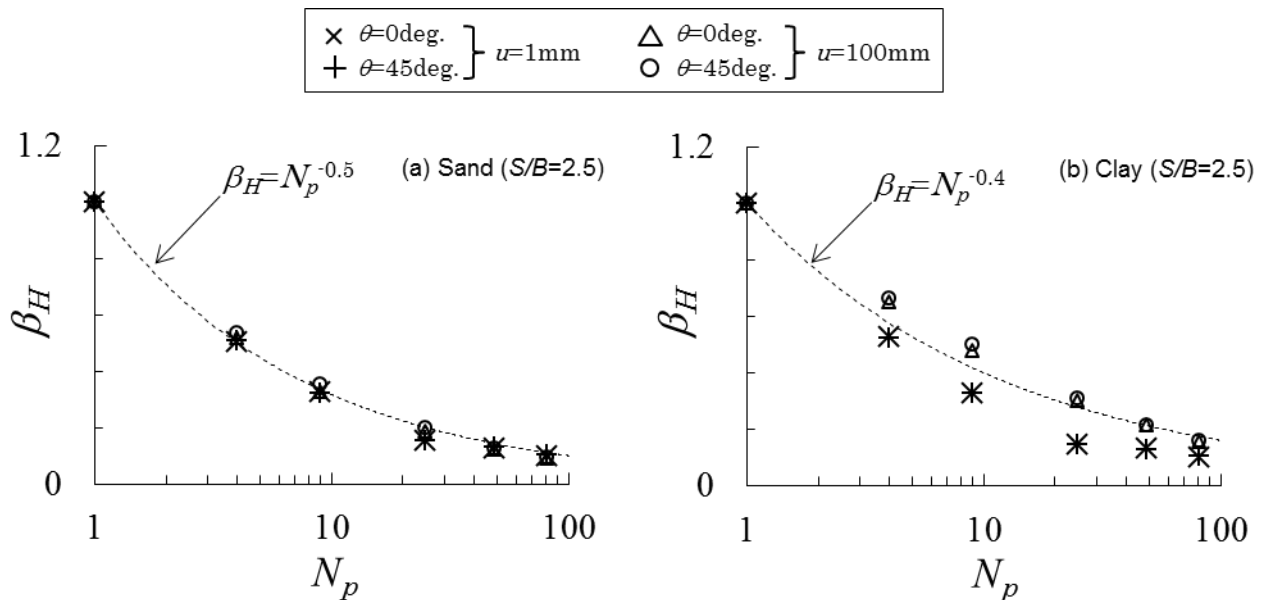


Fig. 6 – Relationship between pile group coefficient of soil springs around the pile shafts (β_H) and the number of piles (N_p) at GL-1.5m

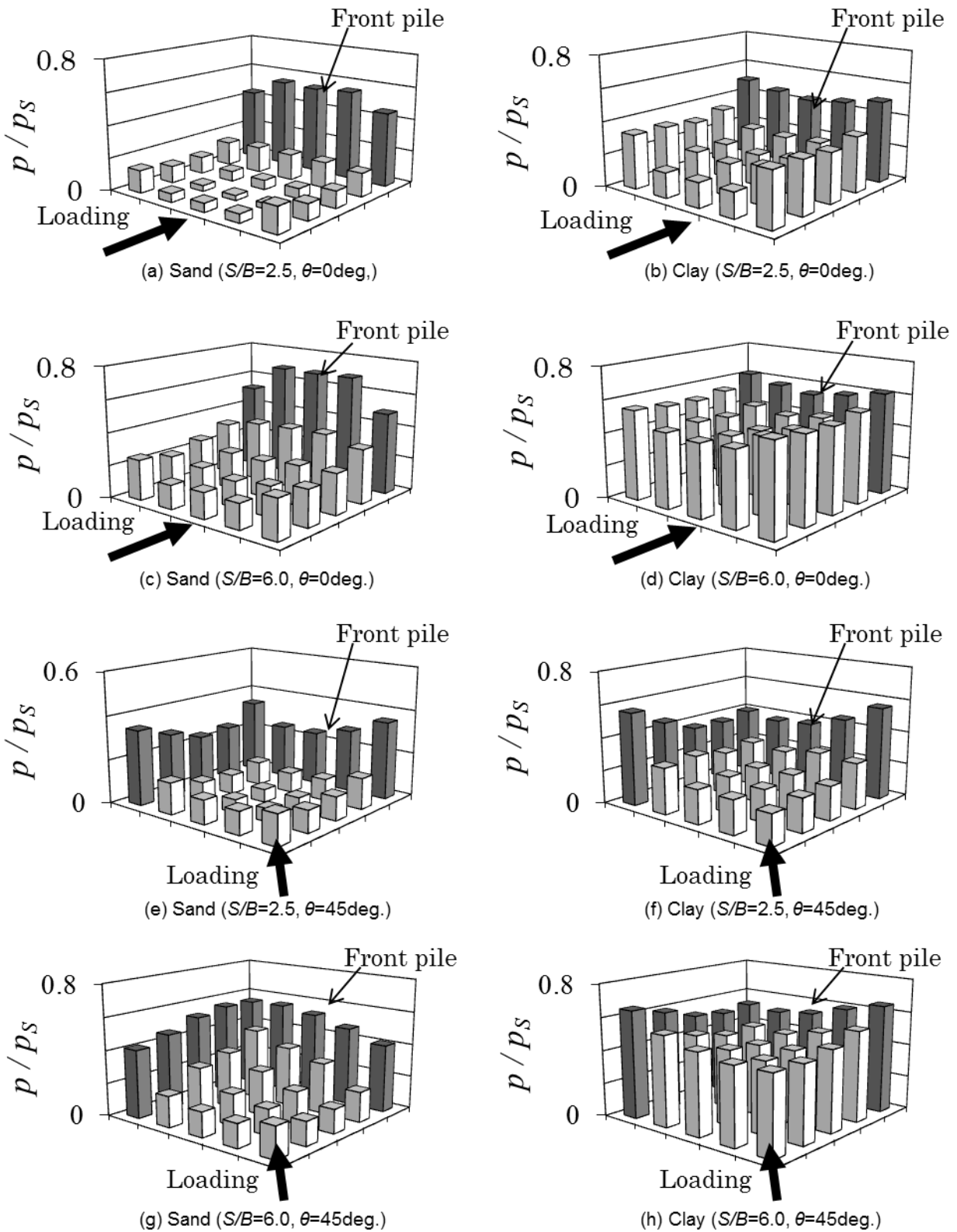


Fig. 7 – Distribution of the subgrade reaction at GL-1.5m
(5 x 5 pile group, $u=100\text{mm}$)

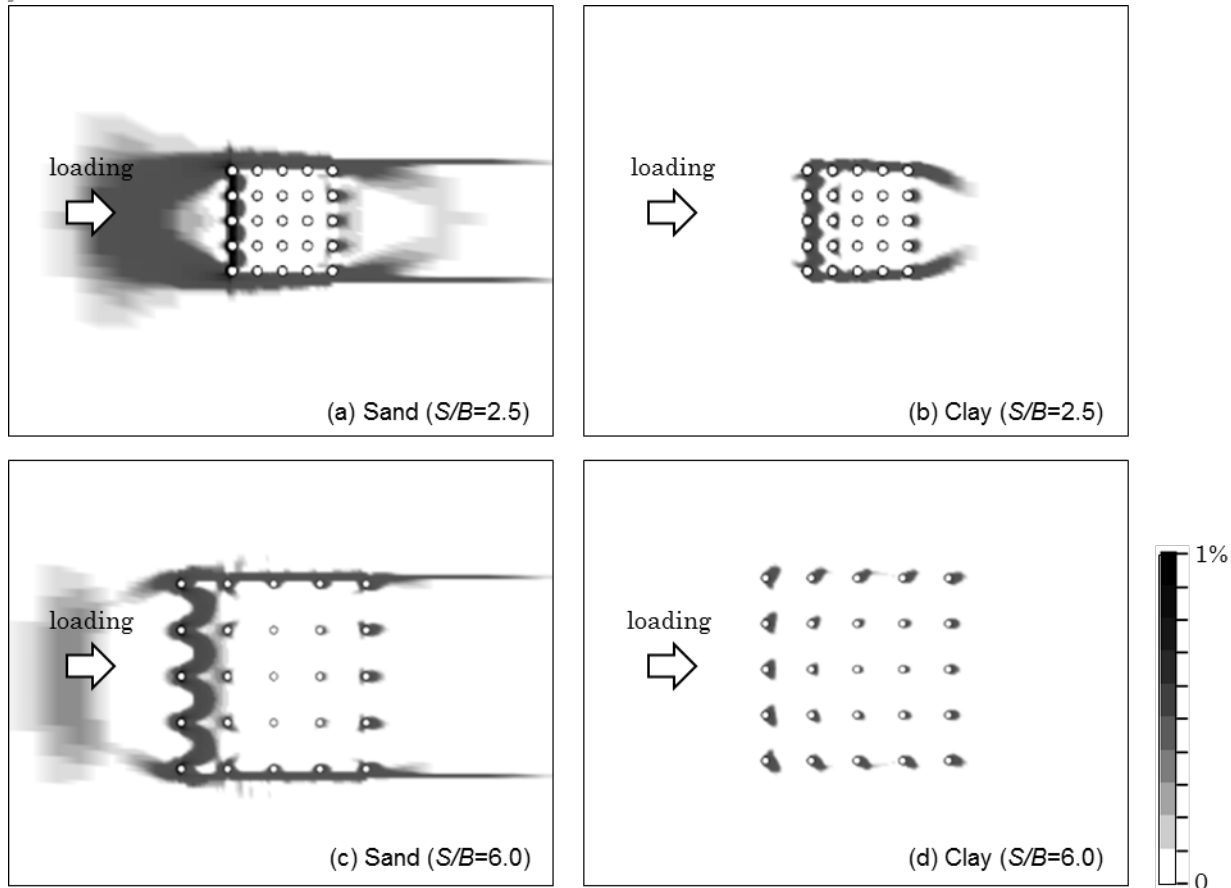


Fig. 8 – Distribution of effective plastic strain in soil at GL-1.5m
(5 x 5 pile group, $\theta=0\text{deg.}$, $u=100\text{mm}$)

Figure 8 shows the distribution of effective plastic strain of the soil of the 5 x 5 pile group subjected to a displacement of 100mm in the direction of 0° . In the cases of a pile spacing of $2.5B$ placed in sand, a pile spacing of $2.5B$ placed in clay, or a pile spacing of $6.0B$ placed in clay, large plastic strain occurred on the edge of the pile group. Only in the case of the pile group with a pile spacing of $6.0B$ placed in clay, plastic stain was observed in front of each pile. Thus, the difference of horizontal soil resistance which depended on the pile spacing and soil type influenced the distribution of the subgrade reaction.

Figure 9 illustrates hysteresis curves of the soil springs along the pile shafts at GL-1.5 m for the single pile and the 5 x 5 pile group, which were obtained from cyclic loading analyses. When the piles were placed in sand, the characteristics of the hysteresis curves of each pile in the pile group were different from that of a single pile. The shape of the hysteresis differed from each other depending on the pile location by the cyclic loading. The subgrade reactions of the front piles were larger than the other back piles. For the B and E-piles in Figure 9 that located in the middle part of the pile group, the hysteresis curves were symmetrically shaped and the hysteresis damping was small. For the A, C, D and F-piles that located on the edge of the pile group, triangle-shaped hysteresis curves could be observed with larger hysteresis damping in the case of front piles. On the other hand, when placed in clay, hysteresis curves of the soil springs were almost symmetric for all piles because the difference of the subgrade reaction between the front piles and the other piles was small as shown in Figure 7. Furthermore, slip behavior in hysteresis loops were observed by the gapping at the pile-soil interface during the unloading direction.

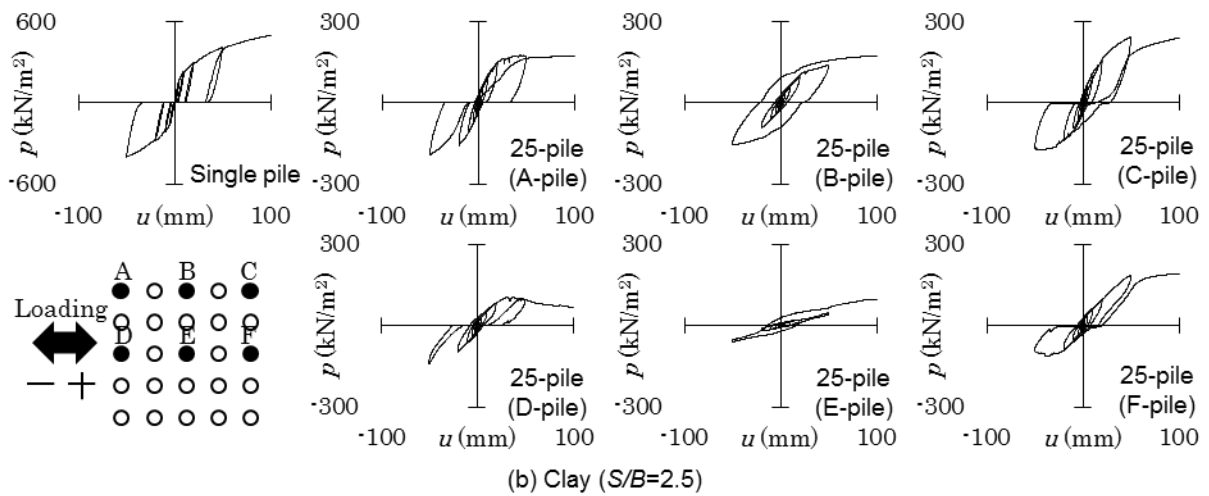
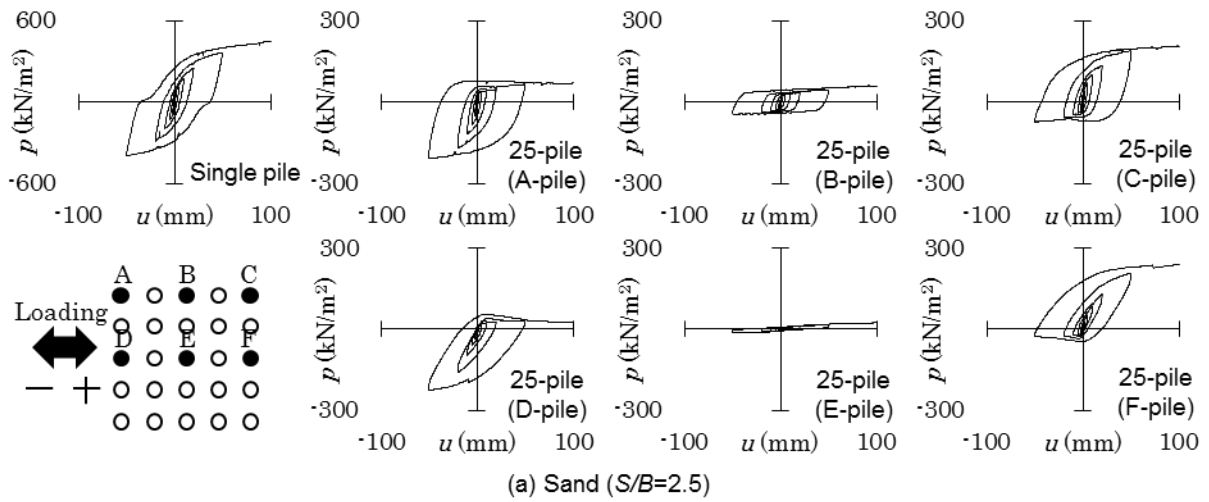


Fig. 9 – Relationship between subgrade reaction (p) and displacement (u) at GL-1.5m during cyclic loading

5. The directivity of springs of each pile

Figure 10 shows the relationship between shear force at the pile head (Q) and the loading angle (θ) at the B, C and E-piles in the group of 5 x 5 piles with a pile spacing of $2.5B$ that was subjected to a displacement of 100 mm. For the B and C-piles that located on the edge of the group, shear force varied depending on the loading angle. For the B-pile, the shear force was particularly large when the loading angle was between 45° and 135° , however it was small when the loading angle was 270° . For the C-pile, the shear force was particularly large when the loading angle was between -45° and 135° , while it was small when the loading angle was 225° . For the C-pile, larger shear force showed on a broader loading angle range than for B-pile. Thus, stress may concentrate more on the C-pile than B-pile. On the other hand, E-pile that located in the middle of the group showed small difference of shear force depending on loading angle.

Figure 11 illustrates the relationship between the subgrade reaction (p) and the loading angle (θ) at GL-1.5 m of the B, C and E-piles in the 5 x 5 pile group subjected to the displacement of 100mm. For the B-pile, a large subgrade reaction could be observed when the loading angle was between 45° and 135° . For the C-pile, when placed in sand, the subgrade reaction became especially large when the loading angle was 45° ; when placed in clay, the subgrade reaction became the biggest when the loading angle was -45° or 135° . The

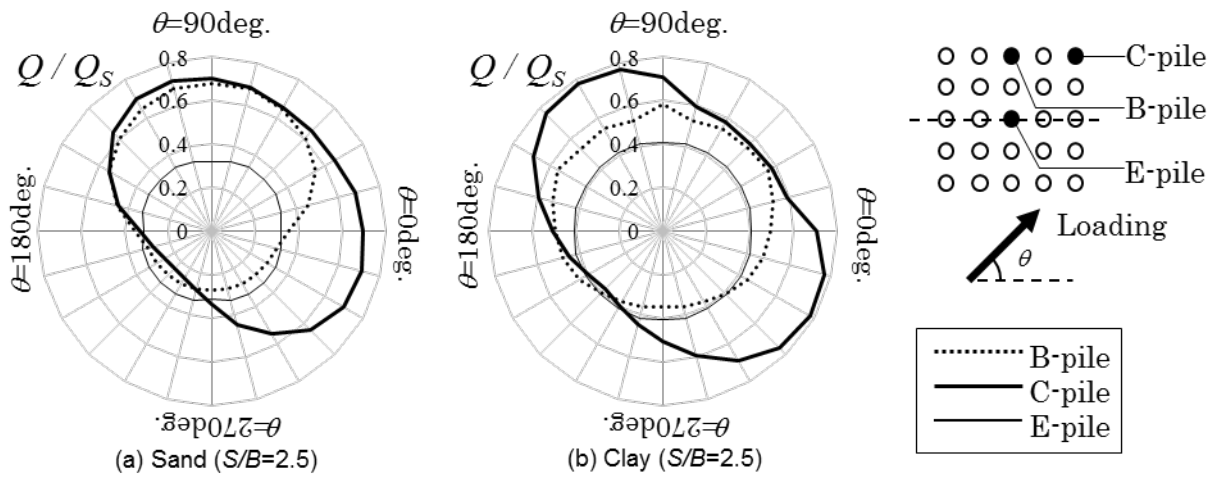


Fig. 10 – Relationship between the shear force at the pile head (Q) and the loading angle (θ) (5 x 5 pile group, $u=100\text{mm}$)

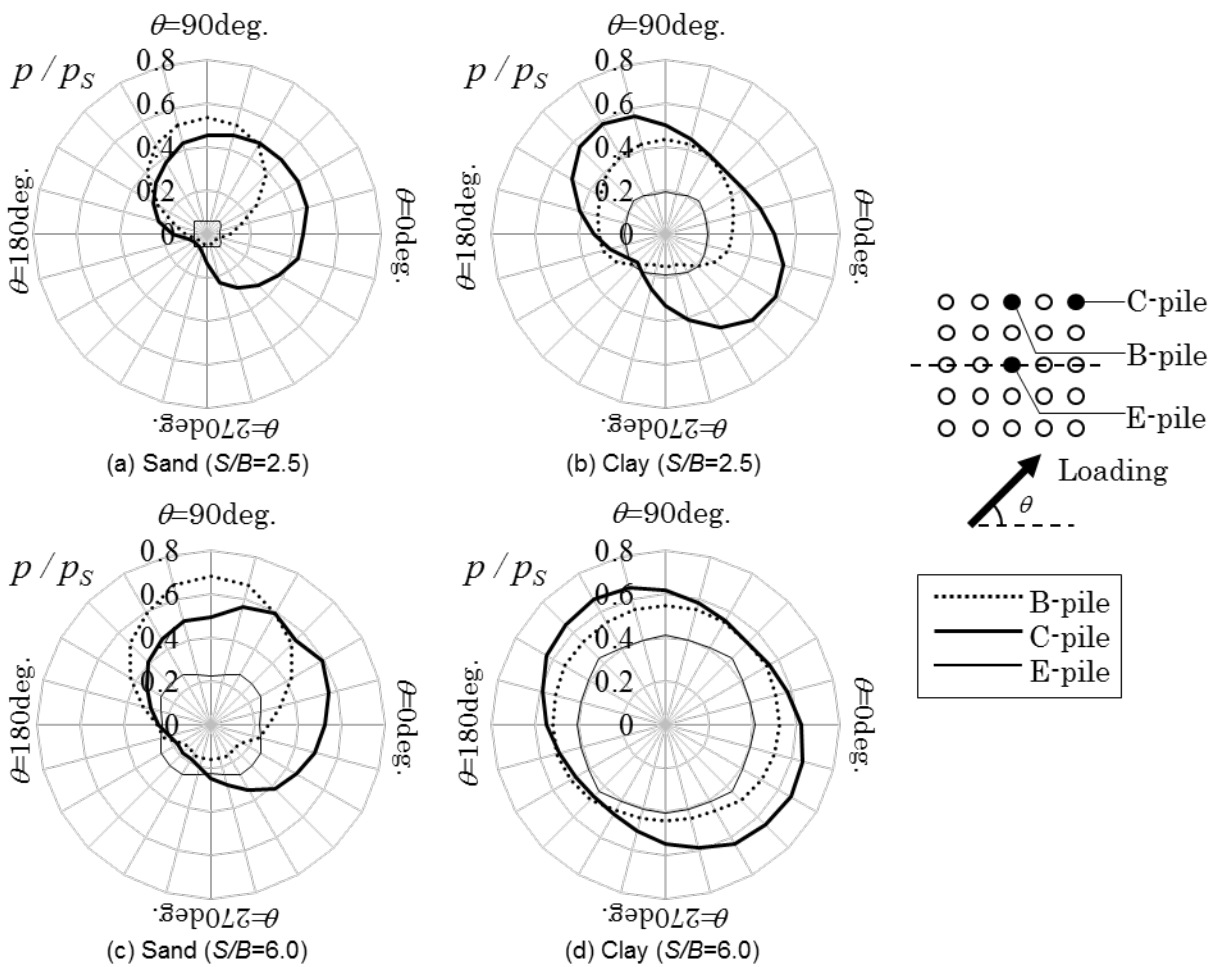


Fig. 11 – Relationship between the subgrade reaction at GL-1.5m (p) and the loading angle (θ) (5 x 5 pile group, $u=100\text{mm}$)



difference of the subgrade reaction based on the loading angle could be seen more clearly when compared to the influence of the shear force, especially in the case of $S/B = 2.5$ or sand. In the case of $S/B = 6.0$ under the condition of clay, the change of the subgrade reaction by the loading angle was small.

6. Conclusion

The major findings obtained from these analyses can be summarized as follows:

- 1) The pile group effect on the subgrade reactions was larger than that of shear forces at the pile head. The number of piles and the soil type affected the pile group coefficient, while the pile displacement and its loading direction had small impact on it.
- 2) The shear force at the pile head and the subgrade reaction along the pile shaft differed depending on the pile location and became larger in the case of the front piles during the loading. These differences could be clearly observed in a pile group with narrower pile spacing in sand.
- 3) For a pile located on the edge of a pile group, the shear force at the pile head and the subgrade reaction along the pile shafts differed depending on the direction of loading. When the pile became a front pile, the shear force at the pile head and the subgrade reaction became larger. These differences could be clearly observed in the pile group with the narrower pile spacing in sand.
- 4) The hysteresis curve of the pile subgrade reaction-displacement relationship located in sand and clay had different characteristics. When the piles were placed in sand, the hysteresis of the pile located on the edge of the pile group showed an asymmetric loop, while those in the middle of the pile group were symmetrically-shaped. When placed in clay, the hysteresis of all piles showed an almost symmetric loop.

7. Acknowledgements

This paper was supported by Grant-in-Aid for JSPS Fellows 26/725.

8. References

- [1] Nakano T, Kashiwa H, Miyamoto Y (2013): Simulation Analysis about Damaged Structure Supported by Piles in Heavily Damaged Zone during the 1995 Hyogoken-Nambu Earthquake. *Journal of Structural and Construction Engineering, AIJ*, Vol.78 No.692, 1695-1704. (in Japanese)
- [2] Kaneko O, Kawamata S, Nakai S, Sekiguchi T, Mukai T (2015): Analytical Study on Damage Factor of Pile Foundations during the 2011 Off the Pacific Coast of Tohoku Earthquake. *Journal of Structural and Construction Engineering, AIJ*, Vol.80 No.717, 1699-1706. (in Japanese)
- [3] Tuzuki M, Inada O, Yamagishi M, Yahata K, Naito Y, Kitamura E (1992): Field testing and analysis of dynamic loaded pile group, 10th World Conference on Earthquake Engineering, Rotterdam, Netherlands.
- [4] Tamaki O, Mitsuhashi K, Imai T (1971): Horizontal Resistance of a Pilegroup Subjected to Lateral Load. *Journal of Japan Society of Civil Engineering, JSCE*, No.192, 79-89. (in Japanese)
- [5] Lemnitzer A, Ahlberg E R, Khalili-Tehrani P, Rha C (2008): Experimental Testing of a Full-Scale Pile Group under Lateral Loading. 14th World Conference on Earthquake Engineering, Beijing, China.
- [6] Kosa K, Suzuki N, Kimura M, Limura Y, Morita Y (1998): Lateral Loading Test of Full-Scaled Pile Foundation Focused on Ultimate Behavior. *Journal of Japan Society of Civil Engineering, JSCE*, No.596, 249-260. (in Japanese)
- [7] Suzuki Y, Adachi N (2003): Relation between Subgrade Reaction and Displacement of Model Pile Based on Horizontal Loading Test. *Journal of Structural and Construction Engineering, AIJ*, No.570, 115-122. (in Japanese)
- [8] Hijikata K, Sugiyama T, Itou M, Fujiwara K, Sako Y, Miyamoto Y (2007): Nonlinear Behavior of Pile-Groups by Experimental and Analytical Study –Vibration Tests of Test Model Supported on 25-piles and Its Simulation Analyses–. *Journal of Structural and Construction Engineering, AIJ*, No.596, 249-260. (in Japanese)



- [9] Kashiwa H, Shouji M, Hayashi Y, Suita K, Kurata T, Inoue W (2008): Influence of Nonlinear Behavior of Pile-Soil Structure on Displacement Amplitude Dependence for Efficiency of Pile Group Based on Cyclic Lateral Loading Tests Subjected to Large Displacement Amplitude. 14th World Conference on Earthquake Engineering, Beijing, China.
- [10] Miyamoto Y, Sako Y, Kitamura E, Miura K (1995): Earthquake Response of Pile Foundation in Nonlinear Liquefiable Soil Deposit. Journal of Structural and Construction Engineering, AIJ, No.471, 41-50. (in Japanese)
- [11] Hijikata K, et al. (2006-2007): Evaluation of Nonlinear Characteristics of Soil-Pile Spring for Pile-Group Structure on the Basis of 3D-FEM Analyses. Summaries of Technical Papers of Annual Meeting (2006), AIJ, 435-440; Summaries of Technical Papers of Annual Meeting (2007), AIJ, 623-628. (in Japanese)